Brazing Stainless Steel Using a New MBF-Series of Ni-Cr-B-Si Amorphous Brazing Foils

New brazing alloys withstand high-temperature and corrosive environments

BY A. RABINKIN, E. WENSKI, AND A. RIBAUDO

Originally Published : Welding Reseach Supplement
February 1998 p 66s - 75s

Electronically Republished: http://www.metlgas.com
Honeywell , 2002

Brazing Stainless Steel Using a New MBF-Series of Ni-Cr-B-Si Amorphous Brazing Foils

New brazing alloys withstand high-temperature and corrosive environments

BY A. RABINKIN, E. WENSKI, AND A. RIBAUDO

ABSTRACT. A group of new high chromium containing amorphous brazing filler metals in foil form has been developed for applications in highly corrosive and/or high temperature environments. These new alloys contain 10–16 wt-% chromium, 1.2–1.6 wt-% boron, *i.e.*, minimal amount needed for amorphability, 7.0–7.5 wt-% silicon, 0–5 wt-% molybdenum, and nickel as the balance. Their T_S is within 975–1030°C (1787–1886°F) and T_L is within 1090–1140°C (1994–2084°F) ranges. The alloys exhibit low erosion of base metal and show no significant detrimental effects on base metal strength because boron concentration is kept to a minimum. It was found that optimal combination of strength, ductility and fatigue resistance of joints is obtained when brazing is combined with high temperature annealing in one extended cycle. The joints after such treatment are practically free of the brittle central eutectic line and the base metals adjoining braze area have only limited and localized segregation of chromium borides. The joint itself is uniform and has a strong and ductile microstructure with only one nickel-chromium-based solid solution phase. The fracture of brazements occurs predominantly in the base metal with the joint ultimate strength higher than the yield strength of the virgin 316L base metal. The brazements have a high corrosion resistance in sea water and water solutions of ammonia and phosphoric acid. This new series of brazing filler metals is currently produced on a regular basis by RS technology as a ductile brazing foil having up to 200 mm width and 50–60 μm thickness. The foil has already been used successfully in brazing of hundreds of large corrosion resistant 316L heat exchangers.

Introduction

Nickel-chromium-based alloys having boron and silicon additions in various concentrations have been used in powder, tape and foil forms as AWS BNi-series of filler metals in joining of stainless steel, heat-resistant alloys, low- and high-alloy steels, etc. (Refs. 1–4). Sometimes these BNi-series filler metals in powder form are used in brazing of plate type heat exchangers that are produced in large numbers for applications in food, chemical, aerospace and other process industries. A standard plate and frame heat exchanger consists of a number of alternating corrugated/flat metal sheets kept in tight, sealed contact with each other by using gaskets or being brazed. An elaborate system of channels is formed by these plates in which two — one hot and one cool — liquid and/or gas media flow separately, exchanging heat and thus saving energy. These plates are mounted on a frame that may be either freestanding or built into a supporting structure. Generally, brazed heat exchangers are stronger and more suitable for high temperature/high pressure applications than those with a gasket-type seal. Fully brazed units have been used for some time with mostly noncorrosive mediums, such as CFCs, HCFCs and HFCs. These brazed units are generally manufactured of stainless steel as the base metal and mostly copper and, in some cases, BNi-series powder as the filler metals.

Recently, because of the hazardous effect on the ozone, a ban on the production of CFCs has caused a great need for development of noncorrosive stainless steel brazes for use with alternative heat exchanger mediums. These brazes should withstand corrosive effect of ammonia and, at the same time, some other even more potent corrosive mediums including sea water, various acid solutions, etc. Brazing alloys for manufacturing such brazes should be compatible with stainless steel base metals and, therefore, nickel-chromium-based filler metals are the best potential choice for such an application. Moreover, of particular importance for heat exchanger performance is the ability of their brazed components to resist fatigue appearing due to alternating thermal stresses. Therefore, brazing filler metals and manufacturing processes associated with them should be chosen to minimize the amount of any brittle phases in such brazes to provide high joint ductility and strength, and high fatigue and corrosion resistance.

Previously developed BNi-series or similar alloys in powder and amorphous form have a few drawbacks. For example, the majority of AWS BNi-series powder alloys contain ≥ 2.75 wt-% boron. It is well known that boron diffuses extensively out of the joint area into stainless steel and superalloy base metals during brazing at high temperatures and forms intermetallic boride phases at grain boundaries. These phases when in large amount are detrimental to base metal mechanical fatigue and corrosion resistance. Large amount of boron in a filler metal may also result in a strong erosion of thin base metal stock of honeycomb structures employed in airfoils and plate heat exchangers. In addition, powder filler metals are not well suited for joining multiple thin plates with a very large total surface area. On the other hand, the existing METGLAS® high chromium, low boron MBF-50 brazing foil having Ni-19Cr-7.3Si-1.5B composition (Refs. 5, 6) cannot be rapidly solidified (RS) into a sufficiently wide (> 100 mm) foil and with thickness higher than 25–30 μm — both needed to manufacture large heat exchangers. These MBF-50 size limitations are due to a negative effect of its high chromium concentration on alloy amorphability.

KEY WORDS

Amorphous Brazing Foil
Stainless Steel Brazing
Brazing
Stainless Steel
Joint Microstructure
Heat- and Corrosion-Resistant Brazing

A. RABINKIN, E. WENSKY, and A. RIBAUDO are with AlliedSignal, Inc.

As a response to these challenges, a group of new amorphous brazing filler metals in a ductile foil form has been developed by precisely optimizing their nickel-chromium-boron-silicon composition and RS casting conditions. These new alloys contain 10–16 wt-% chromium vs. 7 wt-% of existing MBF-20, 1.4 wt-% boron, *i.e.*, minimal amount needed for amorphability, 7.3 wt-% silicon, 0-5 wt-% molybdenum, and nickel as the balance. The major advantage of these new is compositions is that they can be produced as an amorphous foil of sufficient thickness and width to allow brazing of large size parts, despite low boron and high chromium concentration. The new MBF-series of brazing filler metals presented in this paper is currently produced on a regular basis by rapid solidification technology as a ductile brazing foil having up to 200 mm width and up to 50–60 μm thickness.

To optimize brazing conditions for applications of these alloys, a number of different brazing cycles were carried out in which the most perspective alloy of this group, namely Ni-15Cr-1.4B-7.25Si MBF-51, was utilized. The outcome of this research is a set of brazing cycle parameters that yields single phase brazes having a combination of high strength with high ductility.

This paper presents detailed characterization of these new MBF-51 series amorphous filler metals and describes optimal heat treating conditions that result in joints with high tensile strength, and fatigue and corrosion resistance. It also presents in detail and analyzes joint microstructure and fracture surfaces after fatigue and tensile testing of laboratory and industrial specimens obtained under different brazing conditions. Finally, these microstructural data are used to explain mechanisms of joint failure during tensile and fatigue loadings and to propose means for achieving high joint performance.

Materials and Experimental Procedures

Manufacture and Characterization of Ni-Cr-Mo-B-Si Amorphous Foils

The amorphous foils of various compositions were cast first in a form of 12.5 mm (0.5 in.) wide up to 75 μm (3 mil) thick ribbon on a small laboratory unit. Afterwards, manufacturing was scaled up to produce up to 200 mm wide ribbon on a highly productive industrial equipment in multitonnage quantities.

Melting characteristics of these foils were measured using the differential thermal analysis (DTA) method and conducting measurements on a Netzsch STA 429 instrument at 20°C (68°F)/min heating rate in a helium atmosphere. Figure 1 presents a DTA trough of Ni-15Cr-1.4B-7.25 Si MBF-51 alloy as a typical example of its melting behavior. Table 1 shows a breakdown of the compositions and melting parameters of these alloys and other existing Ni-based amorphous brazing filler metals. As one can see, these new alloys exhibit solidus (T_S) within about 975–1030°C (1787–1886°F) and liquidus (T_L) within about 1090–1140°C (1994–2084°) ranges due to low concentration of boron.

The mechanical properties of the as-cast Ni-15Cr-1.4B-7.25Si foil are given in Table 2. In spite of their low plasticity during testing of large specimens, all ribbons with compositions presented in Table 1 are ductile in the as-cast state in microvolumes with dimensions up to a few dozen micrometers, *i.e.*, in order of magnitude of ribbon thickness. Such dual character of ductility is caused by the well-known specific nature of the amorphous state of the metallic alloys. Most importantly, a high ductility on a "micro" scale permits ribbon to bend readily on itself 180° and to be stamped in different configurations without cracking.

The coefficients of thermal expansion, α_T, for amor-

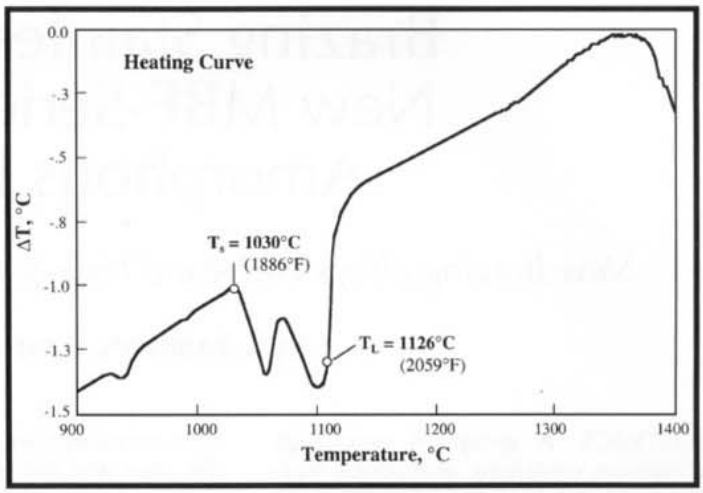

Fig. 1 — DTA melting trough of Ni-15Cr-1.4B-7.25Si MBF-51 amorphous brazing foil.

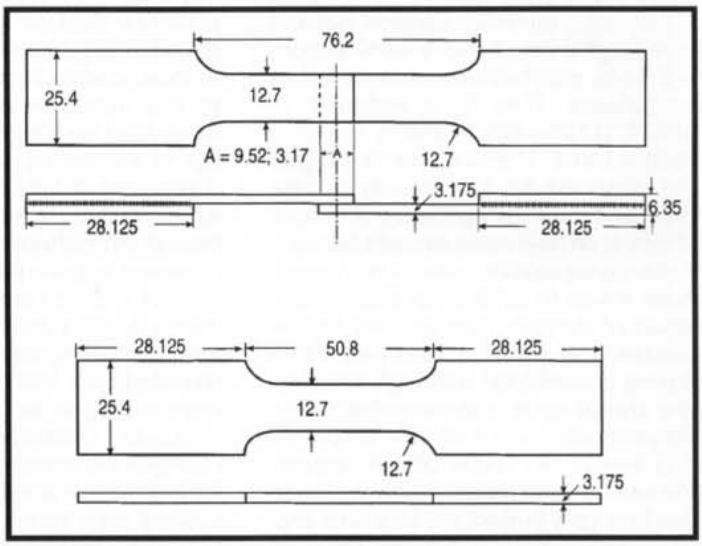

Fig. 2 — Brazed specimens and base metal for tensile and fatigue testing.

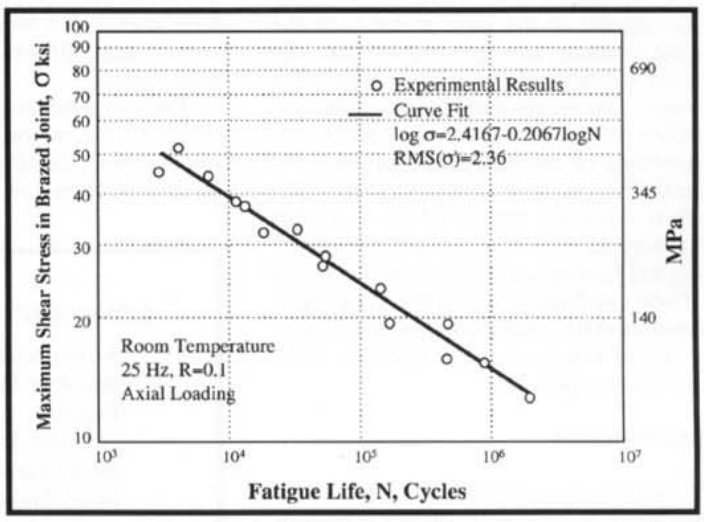

Fig. 3 — S/N fatigue curve for 316L/MBF-51/316L brazed joints.

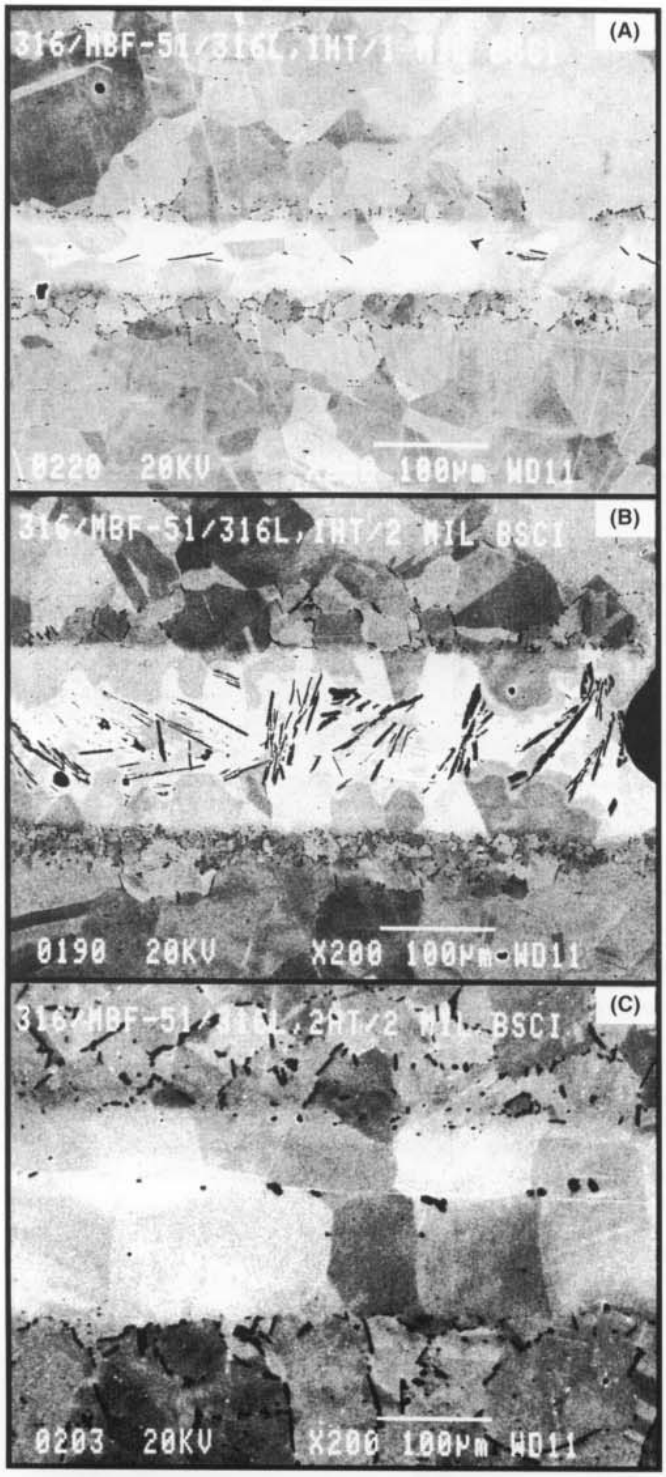

Fig. 4 — SEM micrographs of 316L/316L joints brazed using 1 (A) and 2 (B) mil thick MBF-51 ribbon and a short brazing cycle; 2 mil foil and a long brazing/annealing cycle were used in joint shown in (C). Note that a strong ductile single phase braze was formed when there was a small amount of boron in the joint and/or a long brazing time is used.

phous and crystalline ribbon states are α_T =1.33E-05 grad C^{-1}, very close to α_T of the typical 300 series stainless steel.

Specimen Preparation, Brazing Procedure and Characterization of Brazed Joints

Base metal specimens for all brazability and joint characterization studies were fabricated using 3.175 mm (1/8 in.) thick plates of standard 316L stainless steel. To prepare specimens for brazing, pieces of 25 and 50 µm (1 and 2 mil) thick brazing foil were placed between 25 mm (1 in.) wide 316L overlapping plates and clamped together with these plates thus serving as joint spacers. The clamped assemblies were tack welded slightly on both sides. This welding procedure guaranteed 25 and 50 µm (1 and 2 mil) fix gap joint geometry during brazing. Brazing was carried out in a vacuum furnace under 1.33E-03 Pa pressure with temperature control better than ±5°C (41°F). Table 3 details the time-temperature conditions of the most important trials among all trials that were conducted during this work.

After brazing, specimens for mechanical properties testing were partially machined from both sides to the 12.5 mm (0.5 in.) width to produce specimen geometry similar to that given in American Welding Society AWS C3.2 specification. This machining also removed all traces of the tack welding. After brazing all overlap areas were measured to ensure accuracy in calculation of shear stresses. The specimens for corrosion testing were manufactured in the same way, but from the 25 x 25 x 3.175 mm plates which were overlapped on 12.5 mm. So after brazing, each specimen had two 25 mm long fillets located on opposite sides.

Mechanical properties of brazed specimens were tested using procedures similar to those recommended in AWS C3.2 Specification for the lap type joint configuration. The same type specimens were also used to prepare metallographic specimens. The overlap of specimens for both tensile and fatigue testing was chosen to be equal or smaller than the thickness of base metal plates because of high joint mechanical strength. Otherwise the specimens would be failing only in the base metal thus preventing determination of the joint properties.

The tensile testing was carried out using an "Instron" Series IX Automated 6.04 System instrument at 0.05 in./min crosshead speed. Average tensile, yield and elongation values were determined using a five specimen set for the analysis.

The fatigue life testing of the brazed joints was conducted on an MTS servo-hydraulic test frame with a set of hydraulic wedge grips and using test specimens in a lap shear configuration similar to that shown in Fig. 2. Due to the offset nature of the test specimens, spacer plates of 0.125 in. thick were used to allow correct alignment in the grips of the machine. A sine wave loading cycle was used to evaluate the fatigue life of the specimens. A stress ratio, R, (P_{min}/P_{max}) of 0.1 with a frequency of 25 Hz was used to conduct the testing.

Joint microstructure was observed using optical microscopy and SEM/EDAX analytical methods. A JEOL JXA-840 scanning electron microscope and Noran TN 5500 series II X-ray microanalyzer utilizing IPA57 program were used for SEM analysis. Both WDS maps for light elements and EDS maps were generated.

The fractography of the tested specimens was conducted on a JEOL JSM 6300F field emission scanning electron microscope.

The corrosion testing utilized to evaluate the integrity of 50 µm (2 mil) thick MBF-51 joints was carried out using four different corrosive mediums: a standard sea water solution, a 30% NH_4OH solution, a 25% phosphoric acid solution and 0.5% NaCl and 0.3%$(NH_4)_2S$ solution. Only two mediums, the standard sea water solution and 25% phosphoric acid water solution were used for testing of 37.5 µm (1.5 mil) thick MBF-50 joints due to earlier results from the MBF-51. These results showed that the other two corrosive mediums had little if any detrimental effect on the braze joints (Table 4).

Each braze joint set was manufactured under a single set of time-temperature conditions those considered best for MBF-51 and -50 foil. Each test specimen was thoroughly cleaned with acetone in an ultrasonic cleaner before the test began. Specimens were then removed, dried with dry nitrogen and immediately

Table 1 — Ni-Based Amorphous Brazing Filler Metals

MBF Alloy	AWS and AMS Classsifications	Nominal Composition, wt-%								Melting Temperature		Braze Temperature (Approx.) °C (°F)	Density g/cm³ (lb/in.³)
		Cr	Fe	Si	C*	B	P	Co	Ni	Solidus	Liquidus		
15	—	13.0	4.2	4.5	0.03	2.8	—	1.0*	Bal	965 (1769)	1103 (2017)	1135 (2070)	7.51 (0.271)
20	AWS BNi2/AMS 4777	7.0	3.0	4.5	0.06	3.2	—	—	Bal	969 (1776)	1024 (1875)	1005 (1925)	7.46 (0.270)
30	AWS BNi3/AMS 4778	—	—	4.5	0.06	3.2	—	—	Bal	984 (1803)	1054 (1929)	1085 (1980)	7.94 (0.287)
50	AWS BNi5a	19.0	—	7.3	0.08	1.5	—	—	Bal	1052 (1926)	1144 (2091)	1170 (2140)	7.49 (0.271)
55	—	5.3	—	7.3	0.08	1.4	—	—	Bal	950 (1742)	1040 (1904)	1070 (1960)	7.72 (0.279)
60	AWS BNi6	—	—	—	0.10	—	11.0	—	Bal	883 (1621)	921 (1690)	950 (1740)	7.91 (0.286)
80	—	15.2	—	—	0.06	4.0	—	—	Bal	1048 (1918)	1091 (1996)	1120 (2045)	7.80 (0.282)
51	—	15.0	—	7.25	0.06	1.4	—	—	Bal	1030 (1886)	1126 (2059)	1195 (2183)	7.51 (0.271)
5x	—	10–16	—	7.2–7.4	0.06	1.4	—	—	Bal	975–1030 (1747–1886)	1090–1130 (1994–2066)	—	7.49–7.5

*Maximum concentration.

Table 2 — Mechanical Properties of As-Cast MBF-51 Brazing Foil

Foil Thickness, µm (mil)	Stress at Peak Load, MPa (ksi)	Strain at Peak Load, %	Young's Modulus, GPa (psi)
28.2 (1.11)	1660 (241)	~ 2.0	125 (18 x 10^6)
46.5 (1.83)	1900 (276)	~ 2.0	113 (16 x 10^6)

Table 3 — Tensile/Shear Strength of 316L Joints Brazed Using MBF-51 and MBF-50 Under Various Time/Temperature Conditions*

Brazing Conditions	Thickness of Brazing Foil Used, µm (mil)	Failure Location	Base Metal Stress at Max Load After Brazing, MPa (ksi)	Joint Stress at Max Load, MPa (ksi)
MBF-51 Foil				
(1) Heating to 950°C (1742°F), 60 min hold, + 30 min hold at 1175°C (2147°F), vacuum ~10^{-5} torr. Cooling in N_2 to about 70°C (160°F) for about 30 min.	50 (2) (1.0x overlap)	joint	—	309 (45)
(2) Heating to 1190°C (2175°F), 2.5 h hold, cooling to 1100°C (2012°F), 3 h hold, vacuum ~10^{-5} torr. Cooling in N_2 to about 70°C (160°F) for 30 min.	25 (1) (1.5x overlap)	base metal	504 (73)	>336 (>49)
	50 (2) (1.5x overlap)	base metal	483 (70)	>332 (>48)
	50 (2) (1.0x overlap)	base metal	416 (60)	351 (51)
(3) Heating to 1070°C (1960°F), 20 min hold + 1190°C (2175°F), 30 min hold, vacuum ~10^{-5} torr. Cooling in N_2 to about 70°C (160°F) for 30 min.	25 (1) (1.5x overlap)	base metal	546 (79)	>364 (>53)
	50 (2) (1.5x overlap)	joint	—	149 (22)
MBF-50 Foil				
Heating to 950°C (1742°F), 60 min hold, +30 min hold at1175°C (2147°F), vacuum ~10^{-5} torr. Cooling in N_2 to about 70°C (160°F) for about 30 min.	37.5 (1.5) (1.0x overlap)	joint	—	315 (46)
Flat virgin 316L base metal specimens annealed together with specimens in (2)			Tensile strength, 590 (86) *Yield strength, 199 (29)* i.e., *below joint stress at max load*	

*Specimens similar to AWS C3.2 specimens were manufactured by preplacing 25 or 50 µm (1 or 2 mil) thick ribbon between 1/8 in. thick 316L plates. Ribbons were served as spacers. The plate overlap was 1.5x and 1.0x plate thickness. Afterwards, specimens were tack-welded from both sides to keep the assemblies intact. The tack-welded zones were cut off after brazing to eliminate contaminated areas.

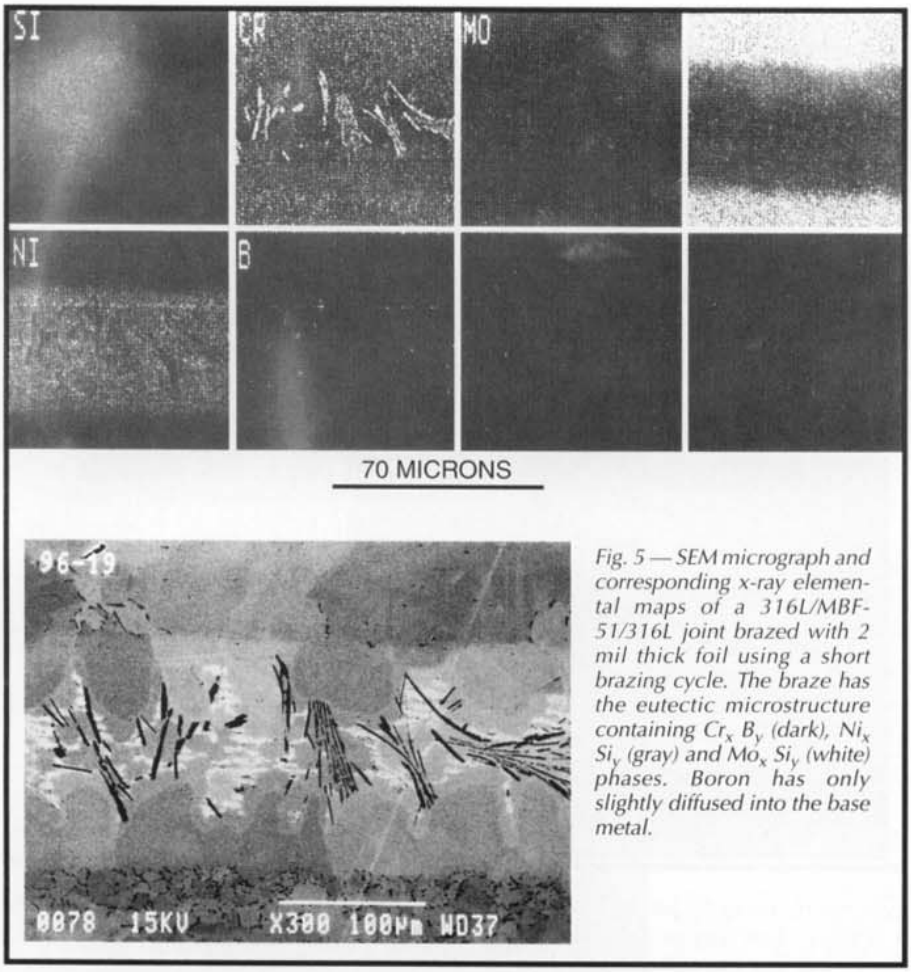

Fig. 5 — SEM micrograph and corresponding x-ray elemental maps of a 316L/MBF-51/316L joint brazed with 2 mil thick foil using a short brazing cycle. The braze has the eutectic microstructure containing $Cr_x B_y$ (dark), $Ni_x Si_y$ (gray) and $Mo_x Si_y$ (white) phases. Boron has only slightly diffused into the base metal.

weighed for the baseline data. Four brazed specimens were then placed in each of six (four MBF-51 case and two MBF-50 case) Pyrex desiccator jars, and each jar was filled with 1500 ml of one of the chosen corrosive mediums. The desiccators were then sealed using a vacuum grease and placed in an oven at 50°C (120°F). Each test specimen remained totally submerged in the test solutions for the duration of the test.

Specimens were subjected to the corrosive solutions for periods of 216, 432, 648 and 864 hours. One specimen from each solution was removed at the designated hour and was cleaned and desiccated until completion of the corrosion testing. At the completion of the testing, all test specimens were weighed, cross-sectioned and polished perpendicular to the main axis of the brazed joint to view the condition of the brazed area. Photographs of the braze joint were taken to document any corrosion effects.

Experimental Results

Brazing Cycle Optimization and Joint Tensile Strength

Conventional brazing with BNi-series filler metals is typically carried out with a holding time at brazing temperature of approximately 15–30 min. Such a short brazing time is insufficient to deplete the braze of silicon and boron via diffusion of these elements into adjoining base metal. Therefore, brittle eutectic intermetallic phases are frequently formed in the joint area upon solidification. The most natural way to avoid this formation is to increase the brazing temperature and holding time during the brazing operation. Alternatively, the appearance of intermetallic phases can also be reduced by using thinner metal foil. In this work we used MBF-51 foils having 25 and 50 µm thickness for time-temperature optimization process because these thicknesses are most often utilized in industry.

To optimize joint structure, more than a dozen various brazing cycles were performed in which both the temperature and time were varied. A post-brazing annealing stage was also added in some of them during the same cycle to provide better braze depletion of silicon and boron. A specimen made using MBF-50 foil having 37.5 µm thickness was also tested as the base line, but only under a single step conventional brazing regime.

The results of tensile strength testing of laboratory specimens are presented in Table 3. As follows from these data, the best process for using a 25 µm (1 mil) thick MBF-51 is a brazing cycle consisting of two short low temperature steps. In this cycle the first 20 min step is made at 1070°C (1960°F), a temperature within the foil melting range and the second 30 min step is at 1175°C (2147°F), a temperature above T_L. Such technological path yields the highest joint strength, > 364 MPa, and the smallest decrease of the base metal strength achieved, namely, from 590 MPa to only 564 MPa. This is attained due to a moderate detrimental effect of boron on base metal. For 50 µm (2 mil) thick MBF-51 foil, a cycle consisting of two consecutive brazing and annealing steps at 1190°C (2174°F) for 2.5 h and 1100°C (2012°F) for 3 h, correspondingly, is a better path. Such a path yields joint strength higher than

Table 4 — Burst Pressure of Four Plate 316L Heat Exchangers Brazed Using 50 µm (2 mil) Thick MBF-51 Foil (Ref. 8)

Process	Process Conditions	Burst Pressure, MPa (ksi)
1	Heating to 950°C (1742°F), 1 h hold + heating to 1175°C (2147°F), h hold + cooling to 1100°C (2012°F), in 1.5 mbar N_2, 2 h hold, and, finally, cooling with furnace in 1.5 mbar N_2	5 (725)
2	Heating to 950°C (1742°F), 1.5 h hold + heating to 1190°C (2174°F), 2.5 h hold + cooling to 1100°C (2012°F), in 1.5 mbar N_2, 3 h hold, and, finally, cooling with furnace in 1.5 mbar N_2	7.1 (1030)
3	Heating to 950°C (1742°F), 1.5 h hold + heating to 1190°C (2174°F), 3 h hold + cooling with furnace in 1.5 mbar N_2	3.2 (464)
4	Heating to 950°C (1742°F), 1.5 h hold + heating to 1190°C (2174°F), 3 h hold + forced cooling in N_2	6.6 (957)

336 MPa and a moderate effect on the stress at maximum load, σmax of the base metal which is in the 504–416 MPa range. Both of these processes produce strength values much higher than 200 MPa yield strength of annealed 316L steel (Ref. 7), *i.e.*, the maximum stress one may apply to any structural part or apparatus made of 316L steel.

In the case of a short 30 min brazing cycle at 1175°C (2147°F), frequently used with 37.5 μm (1.5 mil) thick MBF-50 foil, the failure occured in the joint at approximately σmax = 315 MPa. This value is substantially lower than that of MBF-51 joints achieved after any of the two step brazing cycles applied in this work.

The best brazing regimes discovered in this work were found to be advantageous in brazing of industrial heat exchangers with various sizes. For example, the highest burst pressure of small industrial four plate heat exchangers was achieved when the brazing operation was carried out under the same conditions as those applied in our best cycle for laboratory specimens (Table 4) (Ref. 8). The same was true in other applications dealing with larger heat exchangers weighing hundreds of kilograms. Even with the large size of these heat exchangers, the joint properties were not affected by the lengthy heating and cooling of large industrial oven batches: the brazing part of the total cycle resulted in the best mechanical properties in the case of 50 μm (2 mil) thick MBF-51 foil was sufficiently long to obtain a high strength of various industrial brazements.

Fatigue Resistance

Fifteen specimens were tested for the evaluation of fatigue resistance. The results of this testing are presented in Fig. 3 as the fatigue life plot of the maximum shear stress vs. the number of cycles to failure, N. The fatigue data may be well approximated by a typical linear

$$\log \sigma = 2.4167 - 0.2067 \log N$$

dependence. The results also indicated that MBF-51 joints can sustain shear stress levels at or below 103 MPa (15 ksi) without fracture after more than 10^6 cycles.

Joint Microstructure and its Relationship with Mechanical Properties

Standard 316L/MBF-51/316L Specimens

Figures 4–7 clearly demonstrate the relationships between high mechanical properties and desirable microstructure obtained under the best brazing conditions. The choice of these conditions strongly relates to the total amount of silicon and boron in the joint. That, in turn, is a direct function of the filler metal thickness. For example, according to SEM micrograph (Fig. 4A) a joint produced using 25 μm foil and a short brazing cycle (#3 in Table 3) has practically a single phase microstructure, free from the presence of any brittle intermetallic eutectic phases. The matching X-ray maps show a very uniform elemental distribution in the joint including silicon and boron. On the other hand, the same cycle applied to 50 μm foil joints yielded a pronounced eutectic microstructure inside the joint (Figs. 4B and 5) resulting in lower mechanical strength. This eutectic consists of well shaped $Cr_X B_Y$ intermetallic crystals, $Ni_X Si_Y$ phase and Ni(Fe)-based matrix, with some small additional separate particles containing molybdenum. The composition of these particles was difficult to determine. Both iron and molybdenum appeared in the braze as a result of a substantial base metal dissolution in the liquid filler metal and the affinity of base metal molybdenum to the boron and silicon of the filler metal. The microstructure (Figs. 4C and 6) of the same 50 μm joint after a long term high temperature brazing cycle (#2 in Table 3) looked similar to that of the thin joint after a short heat treating: the eutectic was practically absent and the joint consisted of only a single phase matrix phase with high mechanical strength.

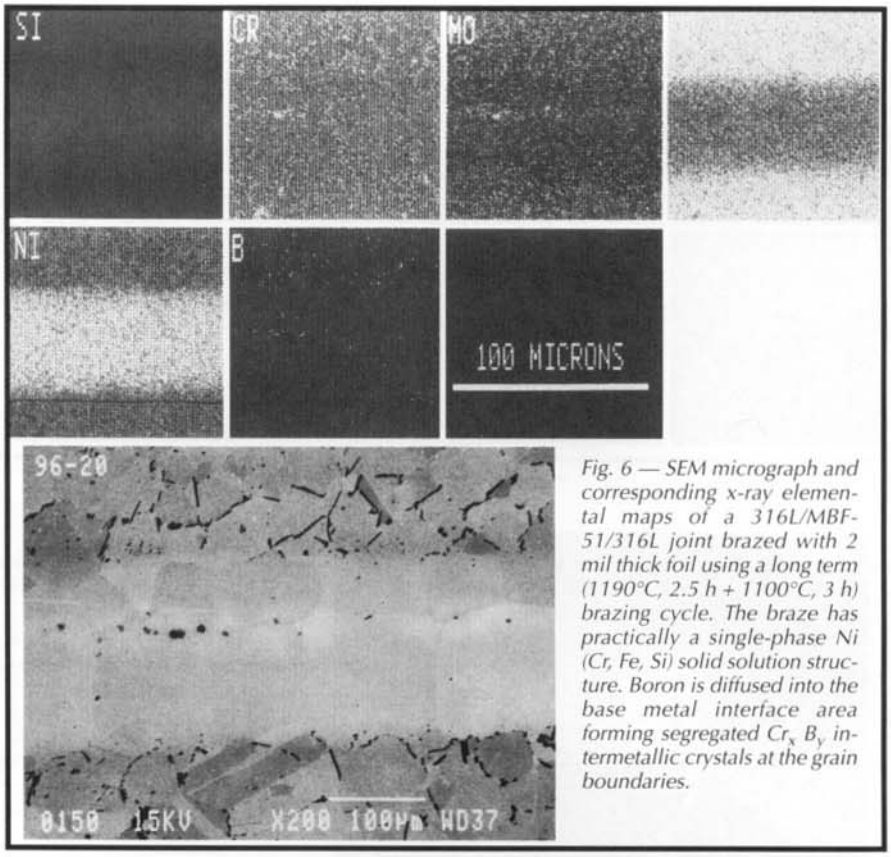

Fig. 6 — SEM micrograph and corresponding x-ray elemental maps of a 316L/MBF-51/316L joint brazed with 2 mil thick foil using a long term (1190°C, 2.5 h + 1100°C, 3 h) brazing cycle. The braze has practically a single-phase Ni (Cr, Fe, Si) solid solution structure. Boron is diffused into the base metal interface area forming segregated $Cr_X B_Y$ intermetallic crystals at the grain boundaries.

The corresponding changes in the base metal microstructures after brazing may be deduced from Figs. 4 and 7. These changes are the appearance of chromium borides at grain boundaries in the joint interface region that affects the base metal strength. Once again, the thinner the braze foil, the less borides would segregate at grain boundaries and the smaller the drop in the base metal strength. A long two step brazing cycle also improved the morphology of borides segregated at the base metal boundaries (Fig. 7): thin extended segregated particles occupying a large part of grain interfaces (Fig. 7B) coagulated into localized rounded ones (Fig. 7C). These rounded particles with a larger volume occupy much less intergranular interface, so important for base metal strength. As a result of this morphological change, the base metal strength after a long term brazing cycle was more than twice that after the short cycle (Table 3).

It is important to point out that a moderate effect of chromium boride formation at grain boundaries of stainless steel on its mechanical properties is well known (Ref. 7). There is a special B-type 300-series of stainless steels for nuclear applications containing up to 2.2 wt-% boron. These are greater in boron content than that in our brazements. In spite of such high boron concentration and ex-

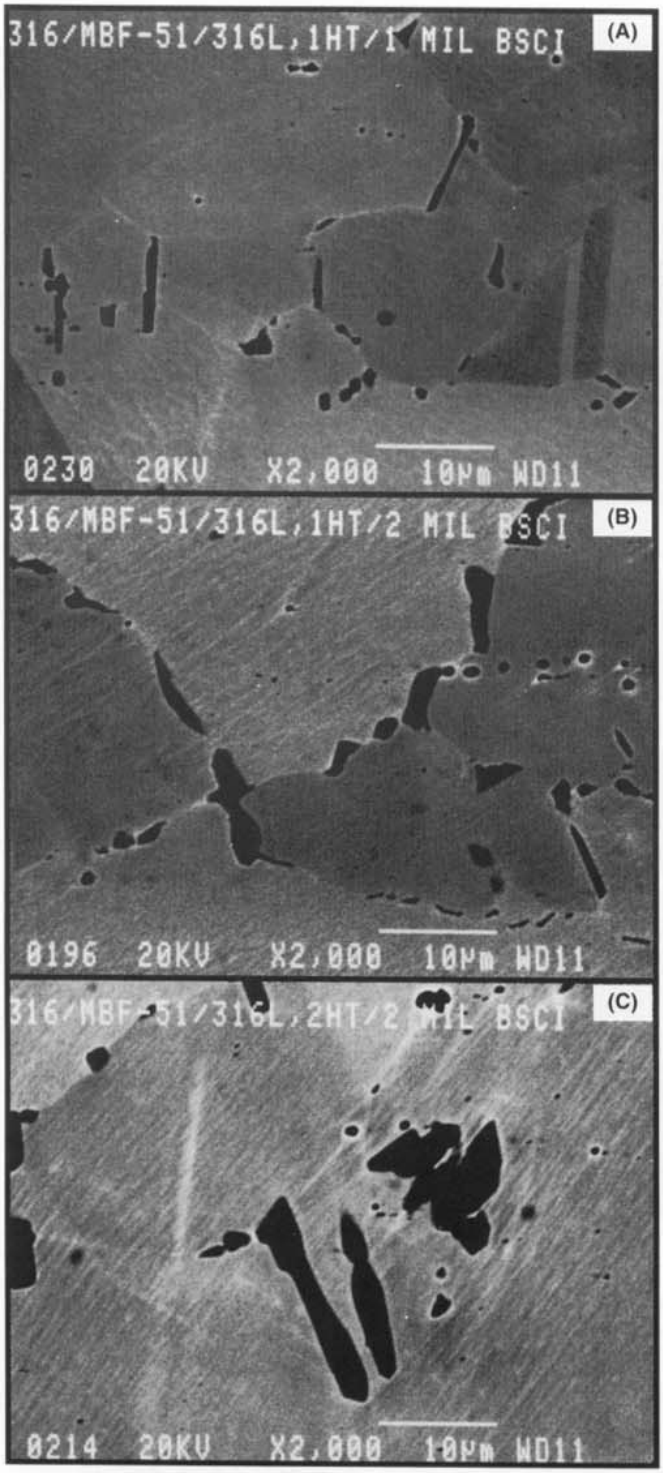

Fig. 7 — SEM micrographs of 316L/316L joints brazed using 1 (A) and 2 (B) mil thick MBF-51 ribbon and a short brazing cycle; 2 mil foil and a long brazing/annealing cycle were used in a joint shown in (C). Note that when either a small amount of boron was present in a braze (A) or a longer brazing time was used with a thick braze (C), boride phases coagulated and did not form the intergranular continuous brittle shells seen in (B).

tensive boride segregation, the yield and tensile strengths of the B-type 300-series stainless steels are 205 and 515 MPa, correspondingly, *i.e.*, only slightly lower than that of the conventional 300-series steel.

Heat Exchanger Joints

A uniform single phase joint microstructure observed in our laboratory specimens can be obtained in industrial brazing as well. Figure 8 shows examples of microstructure of contact areas of two small four plate heat exchangers produced using 50 µm (2 mil) thick MBF-51 foil and brazed applying a short and two step cycles (Ref. 8). A single brazing cycle resulted in the presence of a substantial amount of undissolved brittle chromium borides and silicides of the eutectic structure formed in large fillet areas upon crystallization of filler metal (Fig. 8A). As our observation of failure surfaces shows, these eutectic regions in the fillets were the places where cracks typically originated, thus limiting the performance of these brazed heat exchangers. The reason for such behavior is that usually fillets have a few times larger volume per unit of the base/filler metal interface area than that found inside brazes. Obviously, a longer brazing time is needed to decrease the amount of boron and silicon in fillets. This dissolution via diffusion through the interface should proceed until the boron and silicon concentrations drop below the solubility limits of these elements in the nickel-iron matrix phase. A brazing/annealing cycle applied here (#2 in Table 4), similar to that in our laboratory research, was sufficiently long to accomplish the necessary depletion of boron and silicon even in fillets (Fig. 8B). As a result, the brazements after such a brazing cycle are strong and ductile as the burst testing results presented in Table 5 and the fracture face morphology (Fig. 9) testify.

Tensile and Fatigue Fracture Surfaces and Mechanism of Failures

Figures 9 and 10 show fracture surfaces of failed specimens after tensile/shear and fatigue fracture, correspondingly. The tensile/shear fracture surface shown in Fig. 9 spread through the joint and the base metal regions and had a complex character. In the fillet areas there were numerous features of brittle cleavage of intermetallic particles and adjoining them areas surrounded by features of ductile rupture of the joint matrix phase. In comparison, the fracture surface inside the base metal had ductile rupture features. This transition of the brazement failure from the joint area into the base metal occured because the intermetallic phases were mostly presented in the braze fillets. In these locations, multiple cracks originated first in proximity to these phases and afterwards propagated farther out through the failure region. Since no substantial amounts of intermetallic phases were presented deep in the joint, the fracture then proceeded as ductile rupture of the joint matrix outside of the fillet areas. This rupture then propagated from the joint area into the base metal where the chromium borides are formed at grain boundaries. An additional example of this fracture path is shown in Figs. 11 and 12 depicting a brazed spot of a failed industrial heat exchanger.

The appearance of fractured surfaces after the fatigue failure had practically the same features (Fig. 10) as that after the tensile/ shear failure: a definite combination of brittle cleavage in the fillet areas with ductile rupture inside the joint and the base metal. As in the tensile/shear case, fatigue failures started in the fillet area and then propagated into the base metal of the specimens in a similar way. This effect can also be seen expressively in Fig. 13 showing a specimen partially separated during fatigue testing.

Considering these observations, it may be concluded that the joint strength was above the strength of the adjoining base metal which was affected by brazing process. However, the formation of borides in the base metal caused only a moderate decrease on the base metal strength as denoted in Table 3.

Finally, the important practical conclusion to be drawn from these data is that large volume fillets should be avoided when designing brazed parts and corresponding processing conditions. This can

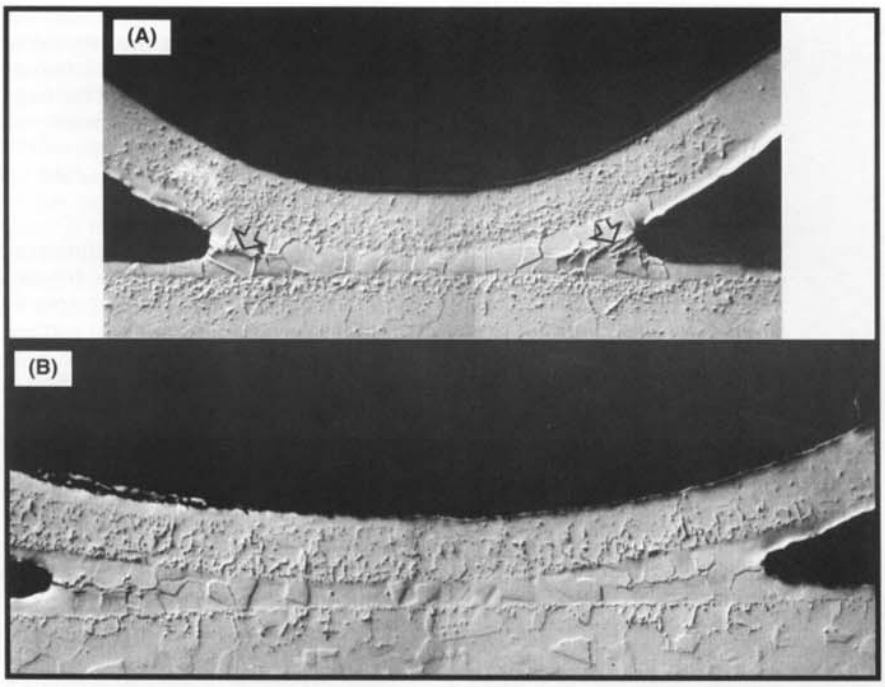

Fig. 8 — Microstructure of brazed spots from two small 316L heat exchangers manufactured using 2 mil thick MBF-51 foil (Ref. 8). A — A short brazing cycle without post-brazing annealing was used. A substantial amount of residual eutectic is present in large fillet areas (arrows) containing brittle eutectic borides and silicides. B — A long brazing/annealing cycle is used. The joint and fillets are practically free from eutectic phases and, therefore, the brazement is strong and ductile.

be achieved by optimizing the geometry of base metal profile and the amount of filler metal supplied to each individual brazement. For example, such an individual optimization of joint geometry in a particular heat exchanger application has resulted in an increase of burst pressure higher than 10 MPa (Ref. 9).

Joint Corrosion

MBF-50 Joints

As seen in Table 5, the weight losses of the test specimens in both sea water and 25% phosphoric acid solution mediums were low. Only sea water produced some visual signs of corrosive pitting attack seen mostly at the joint "beach line" separating the wetted and unwetted areas of the base metal part. This pitting occurred on all of the specimens tested in sea water, with some large pockets of attack on specimens after 648 and 864 h of exposure (Fig. 14).

MBF-51 Joints

In the case of joints brazed with the new MBF-51 foil under conditions giving the highest strength, the weight losses of the test specimens also were low (Table 5). Some corrosion byproducts were seen in specimens from Groups 1 (sea water) and 3 (25% phosphoric acid), but amounted to little, if any, corrosion attack. Scanning electron mocroscope examination of specimen surfaces and cross sections showed little if any corrosion or pitting attack after corrosion exposure (Fig. 15). Some traces of attack also were seen in the base metal on the specimens subjected to the phosphoric acid solution, but generally all the specimens had excellent visual appearance after the corrosion testing.

In general, the corrosion resistance of joints brazed with the new MBF-51 alloy and MBF-50 (BNi-5a) was high. In both cases, the test results showed that the corrosion resistance braze joints was as great as the 316L base metal. It is interesting to note that there was more pronounced pitting corrosion in the MBF-50 joint, in spite of the fact that chromium concentration of MBF-50 foil is 19 wt-% Cr vs. 15 wt-% of MBF-51. A short conven-

Table 5 — Percent Total Weight Loss of 316L/MBF-51 and MBF-50 Joints Subjected to Corrosion Testing in Four Different Medias

S/N	Corrosion Medium	Time in Solution, h	Total Weight Loss, wt-%		Visual Corrosion of Joint	
			MBF-51[1]	MBF-50[2]	MBF-51[1]	MBF-50[2,3]
1-1	Sea	216	0.04	0.006	none	yes
1-2	water	432	0.04	0.058	minor	yes
1-3	solution	648	0.15	0.039	minor	yes
1-4		864	0.21	0.019	minor	yes
2-1	30%	216	0.003	—	none	—
2-2	NA_4OH	432	0.0	—	none	—
2-3	water	648	0.0	—	none	—
2-4	solution	864	0.003	—	none	—
3-1	25%	216	0.49	0.052	minor	none
3-2	Phosphoric	432	0.47	0.097	minor	none
3-3	acid water	648	0.61	0.087	minor	none
3-4	solution	864	0.62	0.088	minor	none
4-1	0.5% NaCl	216	0.0	—	none	—
4-2	and 0.3%	432	0.0	—	none	—
4-3	$(NH_4)_2S$ water	648	0.003	—	none	—
4-4	solution	864	0.0	—	none	—

1. MBF-50 was brazed at 1190°C for 2.5 h and afterwards annealed at 1100°C for 3 h in one cycle.
2. MBF-50 was brazed at 1175°C for 30 min.
3. Some pitting corrosion occurred in the interface area between the outside "beach line" of the fillet and the unbrazed base metal, possibly attributable to too short brazing time of this conventional heat treating cycle.

Fig. 9 — Joint tensile/shear fracture as a combination of 1) brittle cleavage of intermetallic particles and adjoining areas (empty arrows) and 2) ductile rupture of the matrix phase accompanying by formation of cone and shear dimples (curved arrows). Black arrows at the fillet surface show the direction of fracture.

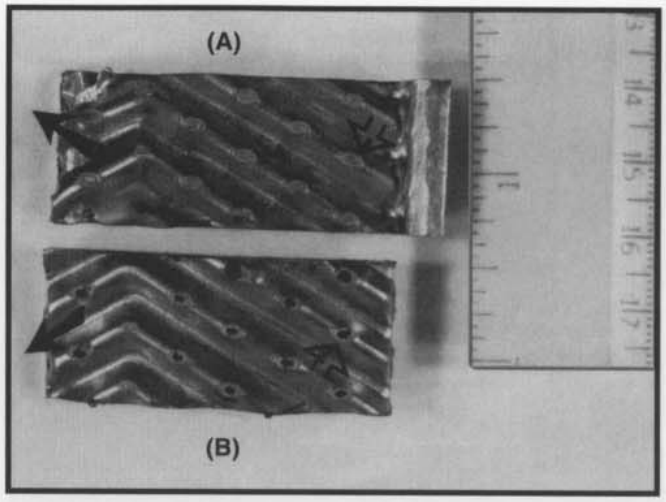

Fig. 11 — Matching parts of a torn apart piece of a heat exchanger manufactured from 316L stainless steel and brazed with the MBF-51 brazing filler metal (Ref. 8). The fracture stresses were applied perpendicular to the plate plane and in the opposite directions. Note that fracture has a mixed mode, i.e., starts in the joint fillet (A) and afterwards propagates into the base metal (B).

Fig. 10 — Fatigue fracture has started in the fillet area in the transcrystalline mode (black arrows) accompanied by formation of multiple cracks. Afterwards it proceeded in the base metal forming numerous striations (empty arrows).

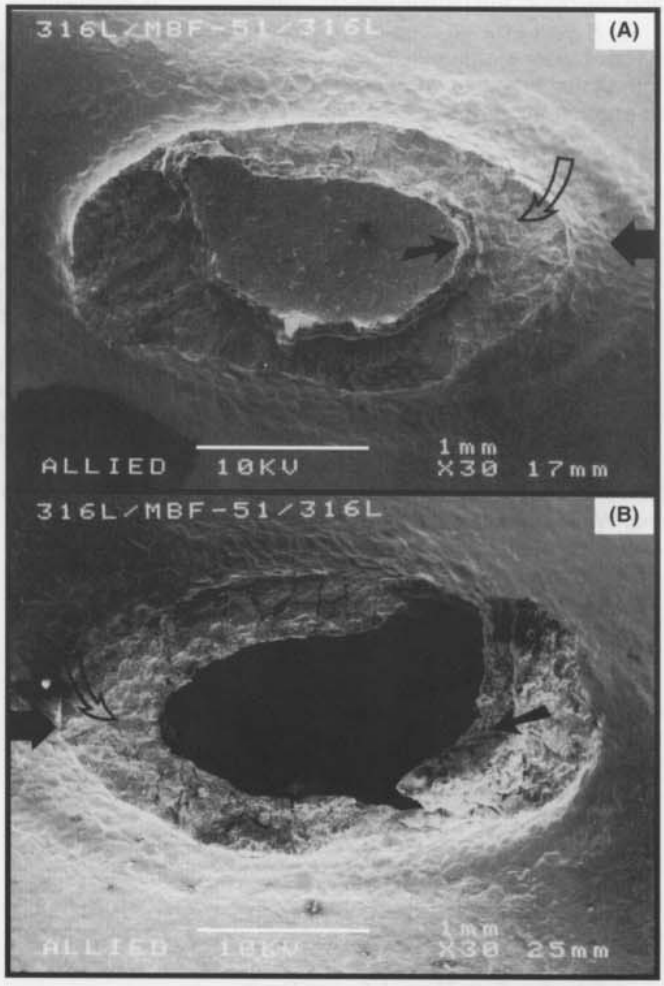

Fig. 12 — Two SEM micrographs of the matching fracture surfaces of a single brazed spot of a torn apart heat exchanger shown in Fig. 11. The fracture direction is indicated by two large black arrows. Fracture started in the fillet area (empty arrows) and afterwards switched to the base metal (small black arrows).

tional brazing cycle time used by these authors for manufacturing the MBF-50 joints is a possible cause of the increased amount of corrosion. The authors believe that a longer brazing cycle similar to that used for the MBF-51 joints may be beneficial for applications with high chromium MBF-50 foil.

Summary

1) New amorphous brazing foil containing up to 15 wt-% Cr, 1.4 wt-% B, 7.25 wt-% Si and sometimes small amount of Mo is introduced for production of stainless steel corrosion resistant heat exchangers and other apparatuses.

2) Single and double step brazing cycles were formulated for application of this new series of Ni-based amorphous brazing foils with various thicknesses resulting in strong, ductile

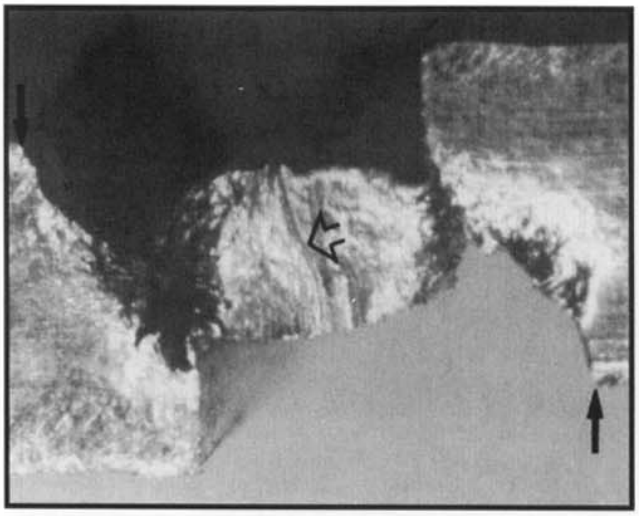

Fig. 13 — A failed fatigue specimen having a geometry similar to that in AWS C3.2. Note that the failure started in the fillet areas (solid arrows) and propagated into the base metal leaving a part of the joint intact (empty arrow). 15X

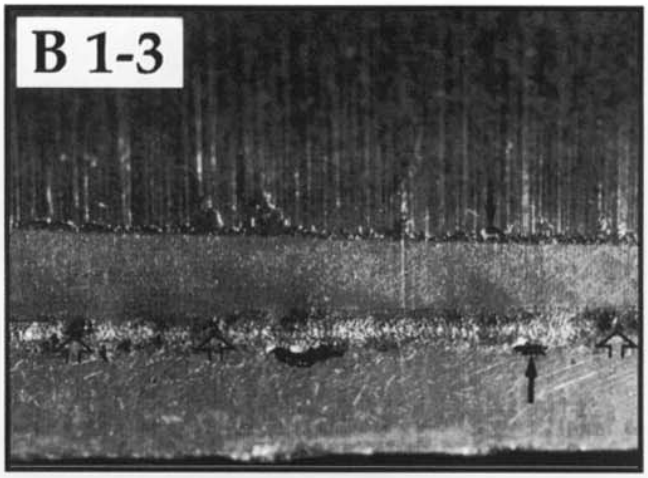

Fig. 14 — A 316L/MBF-50/316L joint after exposure in a standard sea water solution for 648 h. Pitting corrosion occurred in both the base metal (solid arrows) and the braze (empty arrows).

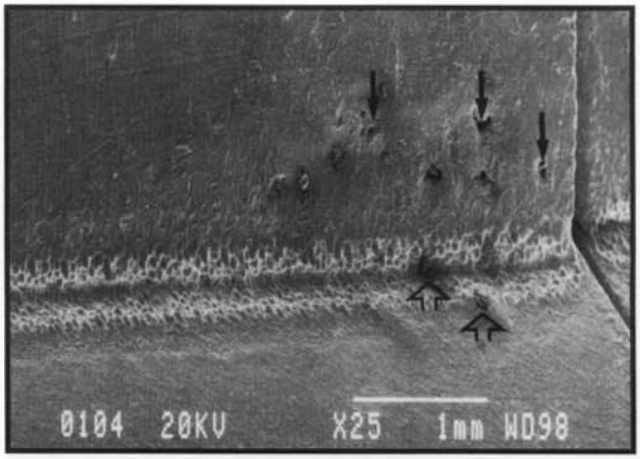

Fig. 15 — A 316L/MBF-51/316L joint after exposure in a standard sea water solution for 864 h. Slight pitting corrosion is seen in the base metal (solid arrows) and the braze (empty arrows).

and corrosion and fatigue resistant joints.

3) A Ni/Cr-based single phase joint microstructure obtained using the best formulated brazing conditions is the key to provide the best combination of joint properties.

4) Because the excelent braze properties have been obtained, the results of this work have been implemented in both the production of new MBF-51 brazing foil and its application on a large industrial scale.

Acknowledgments

The authors wish to thank Messrs. L. Garcia, R. Sancheli, W. Stalzer, W. Majcher, T. Zega for specimen preparation and to B. Sellers for mechanical testing. We are also thankful to Dr. P. Gundel of Industriharderiet in Denmark for providing specimens of brazed parts and kind permission to present data on the burst pressure of tested heat exchangers. Warm thanks are also extended to J. DeTrapano of Bennet Heat Treating Company for the vacuum brazing of all our test specimens.

References

1. Peaslee, R. L., and Boam, W. M. Stainless can be brazed for 2000°F service, *Iron Age*, Sept. 28 and Oct. 5, 1950.

2. *Brazing Handbook*. 1991. AWS, p. 59.

3. ASM Handbook. 1993. Vol. 6 *Welding, Brazing and Soldering*, p. 911.

4. Schaeffer, R. P., Flynn, J. E., and Doyle, J. R. 1971. *Welding Journal* 50(9): 394-s to 400-s.

5. Bose, D., and Freilich, A. 1985. Nickel high chromium-base brazing filler metal for high temperature application, U.S. Patent #4,543,135.

6. Rabinkin, A., and Liebermann, H. H. 1993. *Rapidly Solidified Alloys: Processes, Structures and Properties, and Applications*, pp. 691–736, Ed. H. H. Liebermann, N.Y.

7. Borated stainless steel plate, sheet, and strip for nuclear application, ASTM A pp. 887–889 Standard Specification.

8. Gundel, P. (Industriharderiet, Denmark). Specimens and corresponding test data.

9. Rissler, P. (Private communication).